Transportation Research Part F 66 (2019) 310–323

Contents lists available at ScienceDirect

Transportation Research Part F

journal homepage: www.elsevier.com/locate/trf

# Modelling visual-vestibular integration and behavioural adaptation in the driving simulator

Gustav Markkula [a,*], Richard Romano [a], Rachel Waldram [b], Oscar Giles [a], Callum Mole [b], Richard Wilkie [b]

[a] Institute for Transport Studies, University of Leeds, LS2 9JT Leeds, United Kingdom
[b] School of Psychology, University of Leeds, LS2 9JT Leeds, United Kingdom

ARTICLE INFO

*Article history:*
Received 7 November 2018
Received in revised form 15 April 2019
Accepted 24 July 2019

*Keywords:*
Multisensory integration
Motion scaling
Driver model
Steering
Slalom

ABSTRACT

It is well established that not only vision but also other sensory modalities affect drivers' control of their vehicles, and that drivers adapt over time to persistent changes in sensory cues (for example in driving simulators), but the mechanisms underlying these behavioural phenomena are poorly understood. Here, we consider the existing literature on how driver steering in slalom tasks is affected by down-scaling of vestibular cues, and propose, for the first time, a computational model of driver behaviour that can, based on neurobiologically plausible mechanisms, explain the empirically observed effects, namely: decreased task performance and increased steering effort during initial exposure, followed by a partial reversal of these effects as task exposure is prolonged. Unexpectedly, the model also reproduced another previously unexplained empirical finding: a local optimum for motion down-scaling, where path-tracking is better than when one-to-one motion cues are available. Overall, our findings suggest that: (1) drivers make direct use of vestibular information as part of determining appropriate steering actions, and (2) motion down-scaling causes a yaw rate underestimation phenomenon, where drivers behave as if the simulated vehicle is rotating more slowly than it is. However, (3) in the slalom task, a certain degree of such underestimation brings a path-tracking performance benefit. Furthermore, (4) behavioural adaptation in simulated slalom driving tasks may occur due to (a) down-weighting of vestibular cues, and/or (b) increased sensitivity in timing and magnitude of steering corrections, but (c) seemingly not in the form of a full compensatory rescaling of the received vestibular input. The analyses presented here provide new insights and hypotheses about simulated driving and simulator design, and the developed models can be used to support research on multisensory integration and behavioural adaptation in both driving and other task domains.



## 1. Introduction

Driving simulators can be valuable tools for research on driver behaviour, industrial prototyping of vehicles, and training of drivers (Fisher, Rizzo, Caird, & Lee, 2011), but only as long as the realism of the simulated driving is satisfactory for the application at hand. For this reason, research into driving simulator realism and validity is an active field of work. This is true

* Corresponding author.
*E-mail address:* g.markkula@leeds.ac.uk (G. Markkula).

https://doi.org/10.1016/j.trf.2019.07.018
1369-8478/

not least when it comes to the *motion cueing* in motion-based simulators; i.e., how to best move the simulator within its limited motion envelope, to create a maximally realistic experience of vehicle movement for the driver, and to elicit objective driver behaviour that is similar to that in a real vehicle (Fischer, Seefried, & Seehof, 2016; Salisbury & Limebeer, 2017; Siegler, Reymond, Kemeny, & Berthoz, 2001).

Typical motion cueing algorithms attempt to leverage the properties and limitations of the vestibular (motion) sensory organs in the inner ear, the *otoliths* and *semicircular canals*, and these systems are relatively well understood and have been modelled in mathematical detail (Hosman, 1996; Nash, Cole, & Bigler, 2016). However, much less is known about (i) how drivers then integrate this vestibular information with information from other sensory modalities (e.g., vision) to support vehicle control, (ii) how these processes are affected by the specific nature of the non-perfect motion cues being provided in a given simulator, and (iii) how drivers adapt over time to such imperfections. A quantitative model of driver behaviour that successfully captured such aspects of multisensory integration and behavioural adaptation would be an eminent tool for improving simulators and motion cueing algorithms. The present paper proposes such a model, and tests it against empirical findings from the literature on driving in slalom tasks. Below, the specific aims and structure of this paper will be described, after first providing brief overviews of existing empirical knowledge about drivers' response to down-scaled motion (an important special case of motion cueing), and existing models of multisensory integration and driver steering.

### 1.1. Studies on simulator motion scaling

Most motion cueing algorithms include some element of *linear down-scaling* of the actual motion of the vehicle, to stay within the motion envelope of the simulator, even all the way down to zero motion scaling in fixed base simulators. One often observed effect of down-scaled or zero motion is that drivers adopt more aggressive driving strategies (higher speeds and/or tighter curve-taking; Berthoz et al., 2013; Correia Grácio, Wentink, Valente Pais, Van Paassen, & Mulder, 2011; Jamson, 2010; Siegler et al., 2001), and that the control of the vehicle generally becomes less accurate and more effortful (Berthoz et al., 2013; Jamson, 2010; Repa, Leucht, & Wierwille, 1982). This may however be dependent on the specific driving task, since Wilkie and Wann (2005) found no effect of motion scaling on behaviour in a simple task where participants steered towards a single target.

One type of task where reliable effects have been found, and which is of particular interest in the context of motion scaling, is *slalom* driving. This task is experimentally useful because, when driven at constant or near-constant speed in a simulator, the motion cueing algorithm can be simplified to direct linear scaling only, isolating the effect of motion scaling on behaviour from other types of motion manipulations that are otherwise often applied (e.g., *tilt coordination* and *washout*; Jamson, 2010). Consequently, many authors have studied how driver behaviour in slalom tasks is affected by variations in motion scaling, providing converging evidence for a set of behavioural phenomena: Steering effort, for example measured as steering reversal rates or high frequency steering content, generally increases when motion cues are removed (Correia Grácio et al., 2011; Feenstra, van der Horst, Grácio, & Wentink, 2010; Savona et al., 2014), and task performance, objectively measured or subjectively assessed, generally deteriorates (Berthoz et al., 2013; Correia Grácio et al., 2011), although not always (Savona et al., 2014). Taken together, these findings suggest that in normal driving, drivers integrate visual and vestibular cues, and when vestibular cues are removed, task performance becomes more challenging. However, after repeated exposure to the slalom task, control efforts decrease (Feenstra et al., 2010) and task performance improves (Correia Grácio et al., 2011), suggesting some form of behavioural adaptation over time to the lack of vestibular cues. For motion scaling between zero and one, there are reports from several studies of a local optimum, in the 0.4–0.8 range, where task performance and subjective preferences peak (Berthoz et al., 2013; Savona et al., 2014), and in one case this local optimum was also observed for steering effort (Savona et al., 2014). Different theories have been proposed for why drivers prefer and perform the slalom best at somewhat down-scaled motion cues; here a novel explanation of this phenomenon will be provided, suggesting that it may be a direct effect of multisensory integration.

### 1.2. Models of multisensory integration and steering

There is a large literature on driver steering models (see, e.g., the reviews by Lappi, 2014; Plochl & Edelmann, 2007; Steen, Damveld, Happee, van Paassen, & Mulder, 2011). A recurring theme in this literature has been one inspired from ecological psychology, the study of what exact visual quantities are being sensed and used by drivers (Lappi, 2014), and there has also been a recent surge in interest in modelling steering as *intermittent* control (e.g., Gordon & Zhang, 2015; Johns & Cole, 2015; Markkula, Boer, Romano, & Merat, 2018). However, steering models have typically not considered visual-vestibular sensory integration. In contrast, in the aviation domain, where flight simulators play a very important role in pilot training and certification, there have been substantial efforts to develop multisensory models (e.g., Hosman, 1996; Mulder, Zaal, Pool, Damveld, & van Paassen, 2013; Zaal et al., 2009). In these pilot models, there has been a strong emphasis on *sensory dynamics models*, especially for the vestibular senses. These sensory dynamics models aim to capture how the neural firing rates along afferents leaving the inner ear are transformed compared to the body accelerations and rotations being experienced by the organism (Nash et al., 2016, provide a review). In this type of approach to multisensory modelling, illustrated in Fig. 1(a), the resulting modality-specific internal estimates are then typically combined in linear control laws to model pilot control actions.

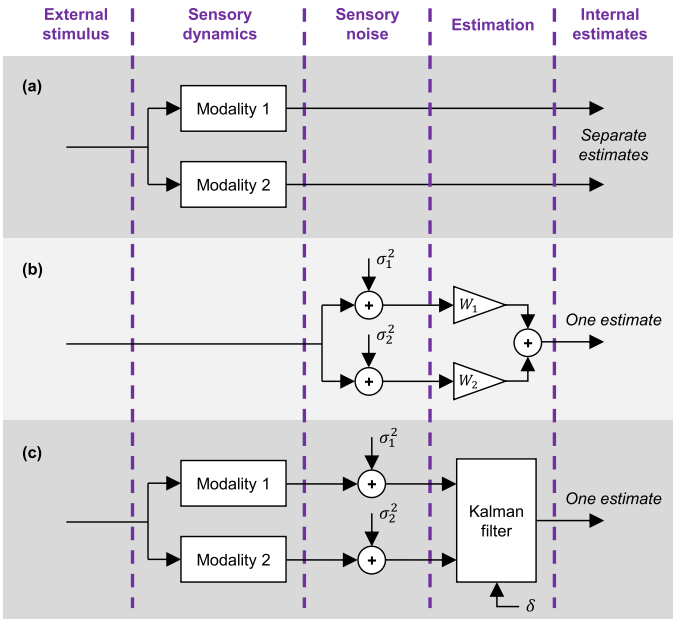


**Fig. 1.** Three different types of modelling schemes for multisensory integration. (a) Sensory dynamics models only; common in aircraft pilot models in research on flight simulators. (b) Modality-dependent sensory noise (variances $\sigma_1^2$ and $\sigma_2^2$) and optimal cue integration; common in psychophysical studies of multisensory integration. (c) Sensory dynamics models, modality-dependent sensory noise, and optimal state estimation, including both optimal cue integration and model-based predictions based on own past behaviour ($\delta$); this scheme is common in optimal control theory models of multimodal sensorimotor control.

In research focusing on perception and psychophysics, on the other hand, the type of model illustrated in Fig. 1(b) has been more common. This model disregards sensory dynamics and instead emphasises the *sensory noise* present in the different modalities; it has been repeatedly shown that humans and other animals often behave as (near-) ideal Bayesian observers, by engaging in (near-)*optimal cue integration*, where the sensory cues are weighted by their reliabilities, i.e., the inverse of their respective noise variances ($W_i \propto 1/\sigma_i^2$ in Fig. 1). Fetsch, DeAngelis, and Angelaki (2013) and Nash et al. (2016) provide reviews of this literature from neurobiological and vehicle control perspectives, respectively.

The model illustrated in Fig. 1(c) is a combination of the models in (a) and (b), with the optimal cue integration being carried out as part of a Kalman filter. This type of scheme has been common in optimal control theoretic models of various sensorimotor control tasks (Franklin & Wolpert, 2011; van Beers, Baraduc, & Wolpert, 2002; van der Kooij, Jacobs, Koopman, & Grootenboer, 1999), and was recently applied by Nash and Cole (2017) in their multisensory optimal control model of driver steering. In these models, the Kalman filter makes use of knowledge of the own past control actions as well as internal forward models of the system being controlled, including the own sensory dynamics. Therefore, as long as any changes in a vehicle's state are mainly caused by the driver's own control, and not by external perturbations such as potholes or wind gusts, the Kalman filter in Fig. 1(c) can compensate for the sensory dynamics, essentially reducing the model to the situation in Fig. 1(b). Since the empirical literature on slalom driving does not emphasise external perturbations, the scheme in Fig. 1(b) will be adopted here.

Predictive forward models, or *generative* models, are also emphasised in so-called *predictive processing* accounts of brain function (e.g., Bogacz, 2017; Friston, 2005). These accounts suggest neurobiologically plausible mechanisms for how the brain can learn its own sensory reliabilities, by first learning a generative model, and then observing deviations between received and predicted sensory data. This type of mechanism will also be leveraged here.

### 1.3. Aims of this paper

This paper proposes, for the first time, a driver steering model that reproduces, and therefore provides stringent and concrete explanations for, the observed empirical effects of motion down-scaling in simulators, specifically (i) how humans first react to down-scaled motion cues, and (ii) how this behaviour changes with repeated task exposure. To address this aim, the model needs to account both for multisensory integration and some form of behavioural adaptation. Here, the neurobiologically plausible framework for intermittent control proposed by Markkula et al. (2018a) was used as a starting point, since it lends itself naturally to a range of plausible potential mechanisms for behavioural adaptation. From a modelling perspective, the novelty lies in the extension of the existing framework with these adaptation mechanisms (as far as we are aware this is the first ever model of behavioural adaptation in steering), as well as with the optimal cue integration mechanisms reviewed

above. It was not an original aim of this work to study the phenomenon of a local optimum in slalom motion down-scaling, but as will become clear below, the model turns out to be applicable also to this phenomenon.

Below, the steering model is first introduced. Then, results from model simulations are presented, before a discussion and conclusions are provided.

## 2. Theory and methods

This section describes the proposed driver steering model, illustrated in Fig. 2, as well as the model simulations carried out to study the model's behaviour.

### 2.1. Driver steering model

#### 2.1.1. Slalom desired path

The model adopts the commonly used concept of a *desired path* (Plochl & Edelmann, 2007) to define the sinusoidal slalom task. The exact setup of this task was here based on (Feenstra et al., 2010): 62.5 m spacing between cones, 3 m lateral amplitude, and the task was carried out at a constant longitudinal speed of 70 km/h.

#### 2.1.2. Intermittent control framework

As mentioned, the model builds on a framework for intermittent sensorimotor control, introduced and described in detail by Markkula, Boer et al., (2018), and schematically illustrated here in the rightmost part of Fig. 2. In brief, this framework assumes that a continuously calculated estimate of currently needed control adjustment $\Delta\delta$ is compared to a prediction of $\Delta\delta$, to yield a prediction error. This prediction error is then fed, with a gain $k$, into an *evidence accumulation* (also known as *drift diffusion*) step where it is integrated over time to a threshold of $\pm 1$, to decide on when a control adjustment is needed. This is in line with neurobiologically proven mechanisms for how the brain makes decisions based on noisy sensory data (Gold & Shadlen, 2007; Purcell et al., 2010; Ratcliff, Smith, Brown, & McKoon, 2016). In the Markkula, Boer et al., (2018) framework, when the evidence accumulation has integrated to threshold, the integrator is reset to zero, a control adjustment is initiated, and a prediction is made of how $\Delta\delta$ will be affected over time by the new control adjustment. The adjustment as such is applied in the form of a kinematic *motor primitive* (Giszter, 2015), here a fixed-duration ($\Delta T$ = 0.4 s, based on the findings by Benderius & Markkula, 2014) stepwise change of the steering wheel angle, with a bell-shaped rate profile and with amplitude obtained directly from the current $\Delta\delta$ prediction error, plus signal-dependent motor noise (Franklin & Wolpert, 2011). Also the $\Delta\delta$ prediction is obtained as a superposition of stereotyped "prediction primitives", mimicking neurobiologically observed *corollary discharge* (Crapse & Sommer, 2008; Requarth & Sawtell, 2014).

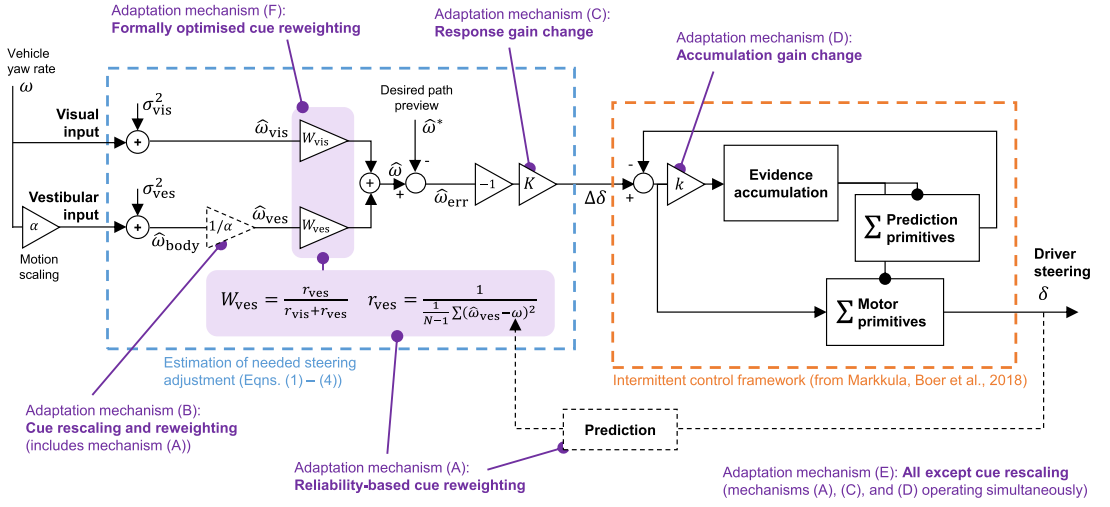


**Fig. 2.** Schematic illustration of the driver steering model tested in this paper. The leftmost part of the figure shows how the model responds to noisy visual and (possibly down-scaled) vestibular cues, creating an estimate of needed steering adjustment $\Delta\delta$ by weighting the modality-specific estimates of the true vehicle yaw rate $\omega$ according to an optimal cue integration scheme (reweighting equations shown only for vestibular weights and reliabilities $W_{ves}$ and $r_{ves}$), and then comparing the integrated estimate $\hat{\omega}$ to a desired yaw rate $\hat{\omega}^*$. The rightmost part of the figure is a simplified illustration of how the intermittent control framework (described in full detail by Markkula, Boer et al., 2018) transforms $\Delta\delta$ into the steering wheel angle $\delta$. The various tested behavioural adaptation mechanisms are also indicated in the figure. The $1/\alpha$ cue rescaling gain is shown in dashed line because it is only present in the model when that adaptation mechanism is enabled; when it is not, $\omega_{ves} = \omega_{body}$. The prediction from $\delta$ to $\omega$ is shown in dashed line because this prediction is assumed in the model without being modelled explicitly; i.e., the prediction-based cue reweighting is using the true yaw rate $\omega$ directly.

*2.1.3. Needed steering adjustment*

In the engineering literature, there are several driver steering models (Gordon & Magnuski, 2006; Markkula, Benderius, & Wahde, 2014; Tan & Huang, 2012) on the general form:

$$\Delta\delta = -K\hat{\omega}_{\text{err}} = -K(\hat{\omega} - \hat{\omega}^*), \tag{1}$$

where $\hat{\omega}^*$ and $\hat{\omega}$ are desired and actual vehicle yaw rate, as perceived by the driver, and $K$ is a steering response gain. As mentioned in the Introduction, there is a considerable literature in the ecological psychology tradition, arguing for the importance of considering what types of information is actually perceptually available to the driver, rather than assuming access to "engineering quantities" like yaw rate. Interestingly however, it can be shown that models in the ecological psychological literature, emphasising more plausible visual inputs such as sight point rotations, can be rewritten on the form of Eq. (1) (Markkula, 2013), so it can be argued that this type of control law is perceptually plausible.

Here, the desired yaw rate $\hat{\omega}^*$ is defined as the yaw rate that would take the vehicle back to the desired path in a preview time $T_P$. This formulation has been shown to successfully replicate human slalom steering, with $T_P \in [1.4, 2.2]$ s (Markkula, Romano, et al., 2018); here $T_P$ = 1.8 s was used.

*2.1.4. Visual-vestibular integration*

As mentioned above, in this paper we follow the psychophysical literature on optimal cue integration, modelling multisensory integration as operating directly on estimates of the external stimulus, in this case vehicle yaw rate:

$$\begin{aligned} \hat{\omega} = \;& W_{\text{vis}}\hat{\omega}_{\text{vis}} + W_{\text{ves}}\hat{\omega}_{\text{ves}} \\ \equiv \;& W_{\text{vis}}(\omega_{\text{vis}} + v_{\text{vis}}) + W_{\text{ves}}(\omega_{\text{ves}} + v_{\text{ves}}), \end{aligned} \tag{2}$$

where $\omega_{\text{vis}} = \omega$ and $\omega_{\text{ves}} = \omega_{\text{body}} = \alpha\omega$, with $\omega_{\text{body}}$ the actual rotation of the driver's body, $\alpha$ the motion scaling being applied, $\omega$ the yaw rate of the simulated vehicle, and $v_{\text{vis}}$ and $v_{\text{ves}}$ being Gaussian white noise with standard deviations $\sigma_{\text{vis}}$ and $\sigma_{\text{ves}}$. Optimal cue integration theory prescribes:

$$W_{\text{vis}} = \frac{r_{\text{vis}}}{r_{\text{vis}} + r_{\text{ves}}}, \quad W_{\text{ves}} = \frac{r_{\text{ves}}}{r_{\text{vis}} + r_{\text{ves}}}, \tag{3}$$

with $r_{\text{vis}}$ and $r_{\text{ves}}$ being the respective sensory reliabilities ($r_{\text{vis}} = \sigma_{\text{vis}}^{-2}; r_{\text{ves}} = \sigma_{\text{ves}}^{-2}$). Note that here, the otoliths and semicircular canals are in effect subsumed into a single estimate of yaw rate, since this is all the control law in Eq. (1) needs (but it may also be noted that in a vehicle, lateral acceleration, as sensed by the otoliths, typically provides good information on yaw rate also).

Thus, overall, what is suggested here (in the leftmost dashed box in Fig. 2) is that drivers might behave as if (i) they transform the neural output from their sensory organs into estimates of yaw rates, presumably considering also predictions based on knowledge of past steering input, (ii) integrate these yaw rate estimates as per Eqs. (2) and (3), and then (iii) compare the result to a visually estimated desired yaw rate, to calculate the needed steering adjustment as per Eq. (1). Note the, "as if" above; it is not assumed that drivers' brains necessarily directly perceive and encode things like desired paths or desired or actual yaw rates, only that they behave as if they do.

Here, $\sigma_{\text{vis}} = 0.5°$/s was used, loosely based on Nesti, Beykirch, Pretto, and Bülthoff (2015), who found that humans could discriminate between visual rotation stimuli of about 5°/s (at which yaw rates typically peak in the present slalom task) if they were different by 1°/s. The 0.5°/s noise level gives 75 % correct direction classification, by a drift diffusion model such as in the intermittent control framework used here, of a 1°/s stimuli if presented during 10 s, a similar duration of presentation as in Nesti et al. (2015).

As for the vestibular noise, the literature on how visual and vestibular sensory systems compare in terms of delays or noise levels provide conflicting information for different types of experimental conditions (Nash et al., 2016), so for simplicity we here assume $\sigma_{\text{vis}} = \sigma_{\text{ves}}$, to begin with. However, later in this paper we also examine the model's sensitivity to variations in these noise levels.

It is assumed that when first entering the simulator, the driver's sensory weightings are preset, based on prior driving experience, in line with the true sensory reliabilities ($r_{\text{vis}} = \sigma_{\text{vis}}^{-2}; r_{\text{ves}} = \sigma_{\text{ves}}^{-2}$), which with $\sigma_{\text{vis}} = \sigma_{\text{ves}}$ gives $W_{\text{vis}} = W_{\text{ves}} = 0.5$.

*2.1.5. Behavioural adaptation*

As also illustrated in Fig. 2, a number of mechanisms for behavioural adaptation are assumed to be operating, alone or in combination:

(A) Reliability-based cue reweighting. In line with the predictive processing models mentioned above, this adaptation mechanism assumes that the driver has a generative model that can predict current yaw rate $\omega$ based on past steering input $\delta$, but this prediction is not modelled explicitly here; the model instead operates on true $\omega$ directly. After each simulation run of the slalom, the perceived noisy visual and vestibular yaw rate estimates $\hat{\omega}_{\text{vis}}$ and $\hat{\omega}_{\text{ves}}$ are compared to the predicted (i.e., true) $\omega$, across all $N$ discrete simulation time steps $i$, to estimate the sensory reliabilities

$$r_{\text{vis}} = \frac{1}{\frac{1}{N-1}\sum_{i=1}^{N}(\hat{\omega}_{\text{vis},i}-\omega_i)^2}$$
$$r_{\text{ves}} = \frac{1}{\frac{1}{N-1}\sum_{i=1}^{N}(\hat{\omega}_{\text{ves},i}-\omega_i)^2}, \quad (4)$$

and the weights $W_{\text{vis}}$ and $W_{\text{ves}}$ are then updated in accordance with Eq. (3) before the next simulation run. As long as there is no motion down-scaling (i.e., $\alpha = 1$), this will just result in the model retrieving approximate estimates of the true inverse noise variances ($r_{\text{vis}} \approx \sigma_{\text{vis}}^{-2}; r_{\text{ves}} \approx \sigma_{\text{ves}}^{-2}$). However, when $\alpha \neq 1$ and $\omega_{\text{ves}} = \alpha\omega$, the estimation of $r_{\text{ves}}$ is affected by the resulting persistent bias of $\omega_{\text{ves}}$ away from $\omega$, causing lower vestibular reliabilities $r_{\text{ves}}$ the further $\alpha$ diverges from unity, i.e., the further the perceived vestibular cues are from what the driver's brain would expect based on its past experiences from real driving.

(B) Reinterpreting the down-scaled vestibular cues, by *rescaling* the mapping from vestibular organ output to $\omega_{\text{ves}}$, i.e., $\omega_{\text{ves}} = \omega_{\text{body}}/\alpha$. Since this type of sensory relearning simultaneously scales up the vestibular noise by $1/\alpha$, it is assumed that it would include appropriate reweighting of cues, i.e., mechanism (A) was also included here.

(C) Adapting the steering response gain $K$, i.e., increasing or decreasing how much one changes the steering angle for a given perceived yaw rate error $\hat{\omega}_{\text{err}}$.

(D) Adapting the gain $k$ in the evidence accumulation. This can be thought of as adapting *effort* or *arousal*; increases in $k$ cause the model to apply more frequent (and hence typically smaller) steering adjustments, and vice versa.

The mechanisms (C) and (D) are assumed to operate so as to optimise behaviour towards some goal, here implemented in practice as an exhaustive search over a grid of the optimised parameters, minimising the cost function:

$$\begin{aligned} J_{\text{tot}} &= k_{\text{path}}J_{\text{path}} + k_{\text{steer}}J_{\text{steer}} \\ &\equiv k_{\text{path}}\frac{1}{N}\sum_{i=1}^{N}(y_i - y_i^*)^2 + k_{\text{steer}}\frac{1}{T}\sum_{j=1}^{n}g_j^2 \end{aligned} \quad (5)$$

for a simulation of duration $T$, with $N$ discrete simulation time steps, in which $n$ discrete steering adjustments with amplitudes $g_j$ are applied, and with lateral positions of vehicle and desired path $y_i$ and $y_i^*$, respectively. This is a common form of cost function for optimal control theory models of steering (Nash & Cole, 2017; Plochl & Edelmann, 2007). Note that it is not implied here that the brain performs grid search to change its behaviour; only that it implements some optimisation mechanism (unspecified here, but see the Discussion) of which the effect is gradual reduction of something like $J_{\text{tot}}$. The weighting parameters were set to $k_{\text{path}} = 1$ and $k_{\text{steer}} = 10$ to get similar magnitudes across both cost function terms in typical simulations with the model. Later in this paper we also examine the model's sensitivity to variations in these weights.

As will be described under Results below, all of the mechanisms (A), (C), and (D) were found promising individually, but not (B). Therefore, also the following was tested:

(E) All three adaptations (A), (C), and (D) operating simultaneously.

Finally, also this mechanism was tested:

(F) Adapting sensory weights not based on estimated reliability as in mechanism (A), but instead to minimise $J_{\text{tot}}$ using the grid search optimisation described above. The purpose of this test was to investigate whether or not the reliability-based cue reweighting (A) yielded similar results as a formal optimisation of the cue weights.

### 2.2. Driver-vehicle model simulations

Simulations were run with a linear vehicle model, fitted to multibody simulations of a Jaguar XF driving slaloms, mostly in the linear tyre regime.

For the gains $k$ and $K$, initial, before-adaptation values for the model were selected as those gains that minimised $J_{\text{tot}}$ for driving with full motion ($\alpha = 1$); i.e., it was assumed that the driver comes to the simulator with these gains preset based on prior driving experience (and can rapidly adapt to the steering gain of the specific simulated vehicle). In practice, an exhaustive grid of values for both gains was searched, with twenty repetitions per gain combination (since the driver model is stochastic) of the $\alpha = 1$ slalom. Optimal model performance was obtained for $k = 450$ (arbitrary units) and $K = 2.04$ s. It may be noted that this latter figure is close to the theoretically optimal steering response gain 1/0.510 s = 1.96 s, with 0.510 $\text{s}^{-1}$ being the steady state yaw rate response gain of the vehicle model used in the simulations.

For motion gains $\alpha \in \{0, 0.05, \ldots, 1\}$, simulations were then first run without any behavioural adaptations, i.e., without any changes to the model parameters. These simulations served to emulate non-adapted driver behaviour during first exposure to down-scaled motion cues. Then, the hypothesised behavioural adaptations (A)–(F) described above were applied, and new simulations were run, to study the impact of these mechanisms on behaviour. For each combination of $\alpha$ and behavioural adaptation (no adaptation or mechanisms (A)–(F)), results were observed across twenty consecutive runs. For all adaptation mechanisms including reliability-based cue reweighting (A, B, and E), the twenty simulation runs from which results were taken, were preceded by runs where the reweighting was allowed to converge from the initial, default sensory weights. It was found that two such simulation runs was enough to ensure convergence.

A number of additional simulated tests were also run, to investigate the model's sensitivity to the difficulty of the slalom in terms of the distance between cones, the assumed sensory noise levels and cost function weights, and the assumption of intermittent rather than continuous steering control. For this latter test, we replaced the intermittent control part of the model (the right half of Fig. 2) with just a fixed time delay of $\Delta T/2 = 0.2$ s and a gain $1/\Delta T = 2.5\ \mathrm{s}^{-1}$, to obtain a continuous rate of steering wheel change $\dot{\delta}$; as explained in (Markkula, Boer et al., 2018) this continuous model behaves roughly as an average-filtered version of the intermittent control model. The steering cost for this model was changed, to consider continuous steering wheel rates instead of discrete steering wheel adjustments as in Eq. (5):

$$J_{\text{steer}} = \frac{1}{T}\sum_{i=1}^{N}\dot{\delta}_i^2,$$

and $k_{\text{steer}}$ was set to 0.1, with the same type of motivation as provided above for the intermittent model.

## 3. Results

### 3.1. Impact of motion scaling and behavioural adaptation mechanisms

#### 3.1.1. Yaw rate estimation

Fig. 3 provides an illustration of the visual-vestibular estimation of yaw rate, from simulations with the model under different conditions. The top panel shows a simulation with full motion cues ($\alpha = 1$), the other three are all simulations with down-scaled motion cues ($\alpha = 0.2$). Note that without any adaptation whatsoever (second panel from top), the combined estimate of yaw rate (black line) becomes strongly biased towards zero, away from the true yaw rate (light gray line). This bias all but disappears when reweighting the cues based on prediction-estimated reliabilities (third panel). If rescaling the vestibular cues (bottom panel), a completely non-biased estimate can again be obtained, making what would seem like a theoretically optimal use of the vestibular cue, despite the vestibular noise also becoming visibly inflated by the rescaling.

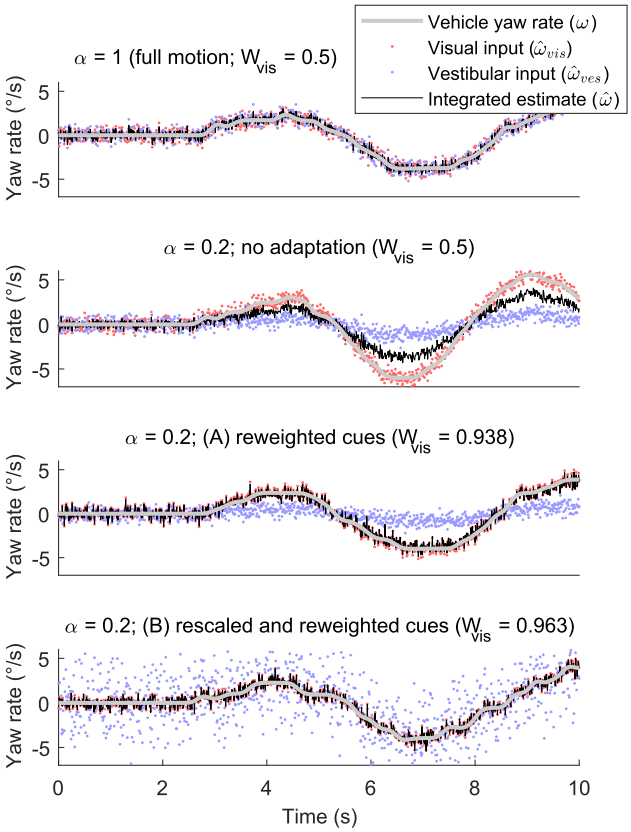


**Fig. 3.** Estimation of yaw rate $\omega$ by the driver model, exemplified by the first ten seconds of four simulations, under different conditions. (A) and (B) refer to two of the adaptation mechanisms described in the text.

*3.1.2. Model time series behaviour*

Fig. 4 shows example time series behaviour of the model in the same four conditions as in Fig. 3. Without any adaptation, the model's steering becomes unstable when motion is scaled down, resulting in increasing path and steering costs. This instability is counteracted when downweighting vestibular cues, both with or without prior rescaling of the vestibular input, but steering efforts still remain higher than in the full motion case. Note, however, that the lowest path cost is obtained for the simulation with reweighted but not rescaled cues.

*3.1.3. Task performance and steering effort*

A more complete overview of path-tracking and steering costs, as a function of motion scaling and adaptation mechanisms, is provided in Fig. 5. It can be noted that, in line with the empirical reports, steering efforts ($J_{steer}$) increase with decreasing $\alpha$, especially for the non-adapted model at low $\alpha$. However, all of the behavioural adaptation mechanisms succeed at improving this situation, which in turn aligns with the empirical reports of decreasing steering efforts after prolonged exposure to the slalom task.

Related patterns can be observed for the path tracking costs ($J_{path}$), but with the important difference that for all simulations except the cue rescaling adaptation (B), there is a local minimum at $\alpha \in [0.6, 0.8]$, i.e., the model reproduces not only the general tendency of worse performance for down-scaled motion, and improvement with adaptation, but also the sub-unity local optimum for motion scaling that has been reported in the empirical literature. After applying the rescaling adaptation (B), however, there is close to zero effect of motion scaling on the model's path-tracking performance.

Analysing the values of adapted parameters provides further insight into how the adaptation mechanisms operate. Fig. 6 shows that the performance improvements from adapting evidence accumulation and steering response gains are both had by increasing these gains, resulting in more frequent adjustments and higher-amplitude steering adjustments, respectively. Fig. 7 shows that the cue weighting obtained by measuring reliability as deviations from expected sensory input, a type of reliability estimate that should be readily available to the brain, was relatively close to the optimal weighting obtained when formally optimising for minimal cost $J_{tot}$.

*3.2. Sensitivity to task and model variations*

Fig. 8 illustrates the model's sensitivity to various modifications to the task and the model itself.

*3.2.1. Slalom difficulty*

Fig. 8a shows that the qualitative behaviour of the model is insensitive to the spacing of the cones in the slalom task. However, the model can be seen to reproduce another empirical observation made by Savona et al. (2014); the motion scaling optimum occurs at lower $\alpha$ for more difficult slaloms (with shorter cone spacing, requiring higher lateral accelerations).

*3.2.2. Sensory noise*

As mentioned earlier, it is difficult to know what magnitudes to choose for the sensory noises. However, as long as $\sigma_{vis} = \sigma_{ves}$, changing these up or down does not change the shape of the path-tracking and steering cost curves; these simply go up and down with the noise levels.

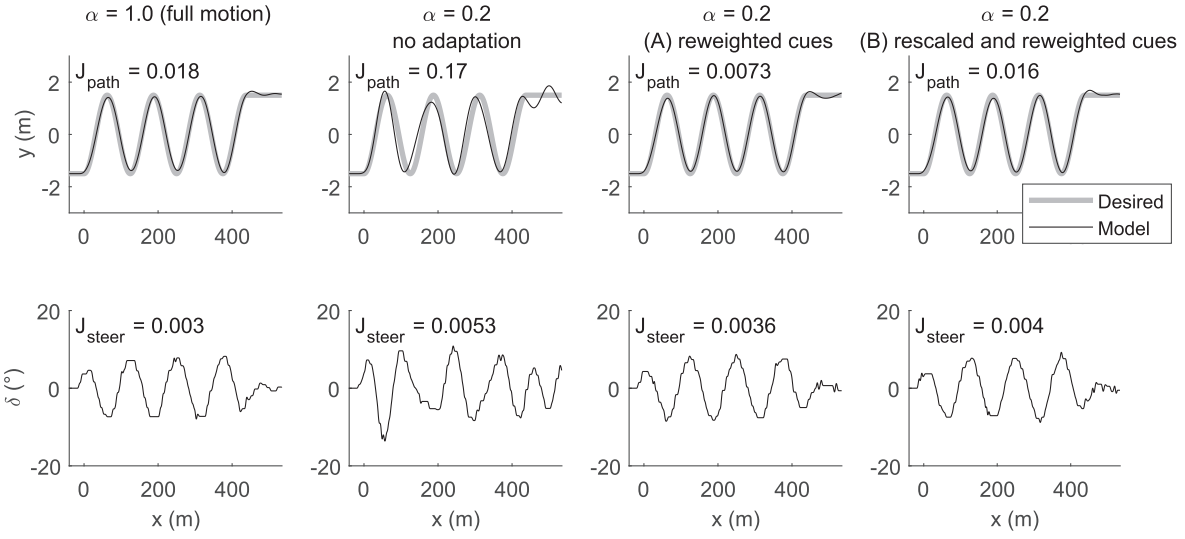


**Fig. 4.** Example time series behaviour of the model in four simulations, under different conditions. The quantities *x* and *y* denote, respectively, longitudinal and lateral distance along the slalom track. (A) and (B) refer to two of the adaptation mechanisms described in the text.

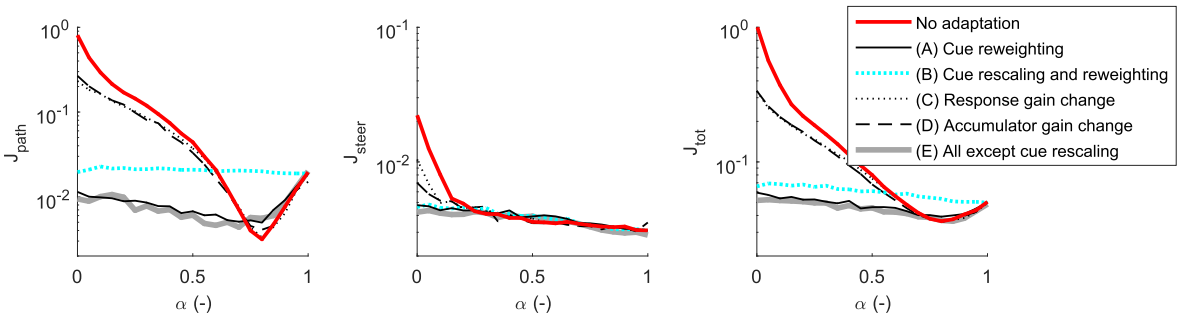


**Fig. 5.** Costs as a function of motion scaling, for the non-adapted model and for the hypothesised adaptation mechanisms (A)–(E).

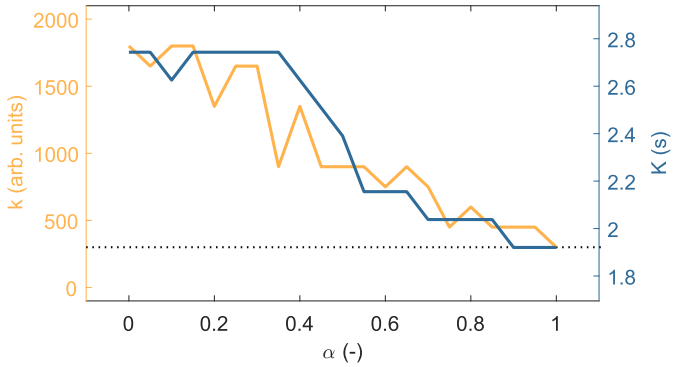


**Fig. 6.** Adapted optimal evidence accumulation gain ($k$) and steering response amplitude gain ($K$), as a function of motion scaling. The dotted horizontal line indicates the optimal gains for full motion ($\alpha = 1$).

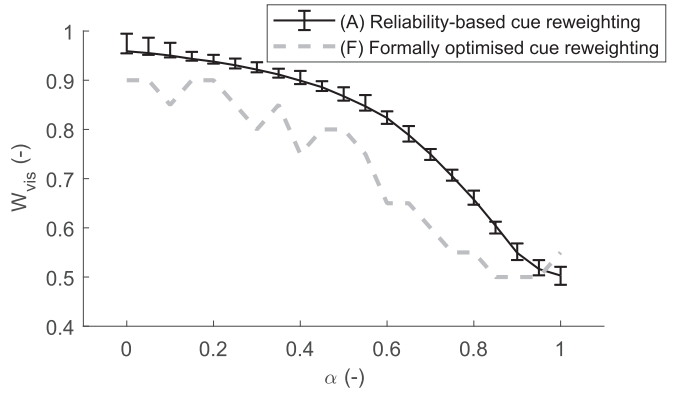


**Fig. 7.** Adapted visual cue weights as a function of motion scaling, estimated from prediction-based sensory reliabilities (shown as average and total spread across twenty task repetitions), and by means of formal optimisation. The vestibular weight is not shown, but is always $W_{ves} = 1 - W_{vis}$.

However, it could be argued, based on perceptual threshold experiments, that the visual system is more sensitive than the semicircular canals in discrimination of pure yaw motion (Riemersma, 1981; Soyka, Giordano, Barnett-Cowan, & Bülthoff, 2012). Therefore, as shown in Fig. 8b, simulations were run where the vestibular noise was increased, while maintaining $\sigma_{vis} = 0.5°/s$. The figure shows that doing so maintains the high-level qualitative effects of motion scaling, but the impact of motion scaling is reduced, in the sense that larger reductions in $\alpha$ are needed to see an impact. The reason the model responds in this way is that with higher vestibular noise levels, Eq. (3) prescribes lower vestibular sensory weights to begin with, making the model less sensitive to variations in $\alpha$. One consequence of this phenomenon is that the local optimum for path-tracking cost shifts to lower $\alpha$ with increased vestibular noise. As mentioned previously, the empirically observed local path-tracking optimum for $\alpha$ is in the 0.4–0.8 range, and the model aligns best with these findings when vestibular noise levels are similar to the visual noise levels (here, $\sigma_{ves} = 0.5°/s$) or up to double the visual noise levels (here, $\sigma_{ves} = 1°/s$).

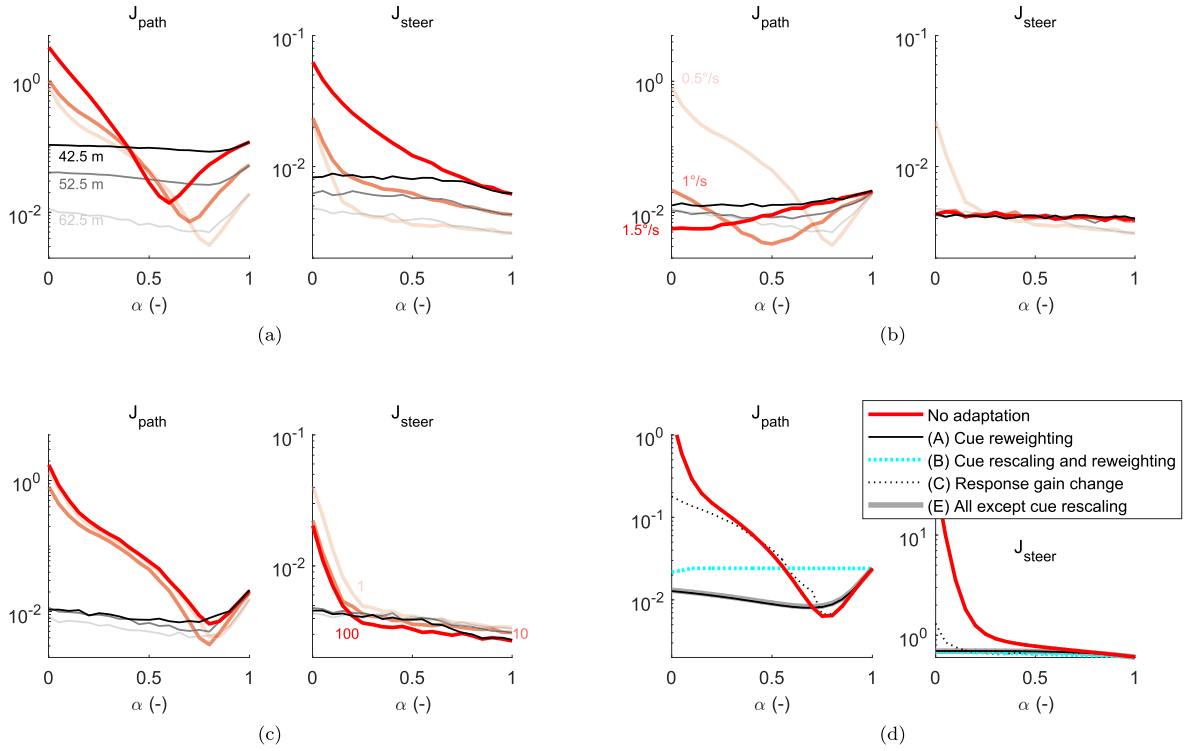


**Fig. 8.** Effects of task and model variations on path-tracking costs $J_{path}$ and steering costs $J_{steer}$, as functions of motion scaling $\alpha$. Note that for readability, panels (a)–(c) show results only for the "no adaptation" and "cue reweighting" conditions. (a) Impact of slalom cone spacing (42.5 m, 52.5 m, or 62.5 m, as indicated in the $J_{path}$ panel). (b) Impact of vestibular sensory noise levels ($\sigma_{ves}$ at 0.5°/s, 1°/s, or 1.5°/s, as indicated in the $J_{path}$ panel; $\sigma_{vis} = 0.5°/s$ throughout). (c) Impact of steering cost weight relative to the path-tracking cost weight ($k_{steer}/k_{path}$ at 1, 10, or 100, as indicated in the $J_{steer}$ panel). (d) Results for a simplified, continuous version of the model. The $J_{path}$ panel retains the scale of the corresponding panel in Fig. 5, but the $J_{steer}$ panel has a different scale due to the different steering cost function. Note that adaptation mechanism (D), accumulation gain change, is not applicable to the continuous model.

### 3.2.3. Cost function weights

The cost $J_{tot}$ is only used to identify optimal model parameterisations, disregarding the actual value of $J_{tot}$. Therefore, modifying both cost functions weights $k_{path}$ and $k_{steer}$ up or down by the same factor does not affect the obtained results, but varying them relative to each other does. However, Fig. 8c shows that this impact is small, even when modifying the ratio $k_{steer}/k_{path}$ by as much as a factor ten up or down (from the original $k_{steer}/k_{path} = 10$). With larger $k_{steer}$, the initial model optimisation (for $\alpha = 1$) yields a parameterisation with higher accumulator gain $k$ and lower response gain $K$, thus applying smaller steering corrections more often, which brings down $J_{steer}$ slightly, at the cost of a small increase in $J_{path}$. As can be seen in Fig. 8c, the qualitative effects of then reducing $\alpha$ and applying adaptation mechanisms remain largely unaffected by the $k_{steer}/k_{path}$ ratio.

### 3.2.4. Continuous model

Comparing the results for the continuous model in Fig. 8d to those for the intermittent model in Fig. 5, it can be seen that many but not all of the qualitative phenomena are retained in the continuous model: Steering costs still go up for the non-adapted model with $\alpha < 1$, and the sub-unity motion scaling optimum for path-tracking persists, but for the continuous model there is close to zero effect of $\alpha$ on steering costs after all of the adaptations.

## 4. Discussion

### 4.1. Sensory integration and behavioural adaptation

The model of multisensory integration used here was relatively simple. Nevertheless, the main targeted empirical phenomena, in terms of task performance and steering efforts, were all qualitatively captured by the model. Thus, the model analyses provided here suggest that low task performance and high steering efforts upon first exposure to down-scaled motion cues can be understood as drivers responding to these down-scaled cues as if they are *directly underestimating vehicle yaw rate*, and use this underestimation when shaping their steering. As a result, this steering becomes more effortful, and in many cases also more unstable.

The fact that the analyses support the idea of drivers using the underestimated yaw rates as part of their control is interesting in its own right. Much of the existing empirical literature on driving simulator motion can be interpreted conservatively in this sense, to say that motion cues mainly cause drivers to change their higher-level strategy in terms of adopted speeds or trajectories, to avoid experiencing large accelerations (Berthoz et al., 2013; Correia Grácio et al., 2011; Jamson, 2010; Siegler et al., 2001), or that motion cues mainly support rejection of unexpected external perturbances like wind gusts (Greenberg, Artz, & Cathey, 2003; Repa et al., 1982). The present model and simulation analyses, together with the existing empirical findings from slalom experiments, instead suggest a stronger account, whereby drivers make direct use of vestibular information as part of shaping their steering to reach their intended targets, also in the absence of any external perturbances or high-level adaptations of trajectory or speed. It is clear that existing multisensory models of drivers (Nash & Cole, 2017) and pilots (e.g., Mulder et al., 2013) also suggest this deep form of involvement of vestibular cues in control, but we are not aware of any prior analysis of empirical data providing support for it in driving.

With respect to behavioural adaptation, the results presented here indicate that especially three mechanisms, or several of them in combination, are candidates for causing the empirically observed effects of repeated task exposure: increased gains in evidence accumulation (mechanism D) or steering response (mechanism C), or sensory cue reweighting based on reliabilities inferred from deviations between received and predicted sensory input (mechanism A). Especially this latter mechanism seems readily implementable in neural systems, and it also provided the most dramatic performance improvements. Interestingly, the cue weights obtained in this way came close to the formally optimal values (mechanism F; Fig. 7); that this would be the case was not clear a priori, since the formally optimal values depend on the specific task and chosen cost function.

Also the increases in accumulator and steering gains can actually be interpreted in neurobiological terms; increases in global cortical arousal by means of broad diffusion of noradrenaline (also known as norepinephrine) has been found to have the specific effect of increasing gains in neuronal response to inputs (Aston-Jones & Cohen, 2005). Thus, it could be hypothesised that the driver's brain may respond to unsatisfactory task performance with release of noradrenaline, increasing the evidence accumulation and response gains.

The present analyses do not provide any conclusive insight into which of the three adaptation mechanisms mentioned above may have been more important in the empirical studies, or whether they were maybe all present simultaneously (mechanism E). However, the results can be taken to suggest that complete rescaling of the vestibular input (mechanism B) may not have occurred in the human drivers in these studies, since if so there would not, according to the model simulations, have remained any local optimum in task performance for $\alpha < 1$. This leads on to the next section.

### 4.2. Sub-unity optimum in motion scaling

It was not expected beforehand that the model would exhibit the local performance optimum for sub-unity motion scaling. Previously, it has been proposed that this phenomenon might be due to imperfections and false cues in motion systems becoming more prominent at $\alpha$ too close to 1, or to motion down-scaling being needed to ensure coherence with underestimated visual speeds (Berthoz et al., 2013), or to successful control of arms and steering wheel becoming more difficult when the body is subjected to higher and more uncomfortable accelerations (Savona et al., 2014). However, none of these mechanisms were included in the model, yet it still reproduced the phenomenon.

Here, what is happening instead is that the model gets a path-tracking benefit from slightly underestimating the yaw rate in this task. Looking closely at the different vehicle trajectories in Fig. 4, or the magnified view in Fig. 9, it can be seen that (i) the path tracking cost is to a large extent determined by how well the vehicle's path is phase-aligned with the desired path, (ii) for $\alpha = 1$, the vehicle trajectory phase is slightly late (reaching apex after the desired path does), and (iii) motion down-scaling shifts the vehicle trajectory to progressively earlier phase, giving rise to the local path tracking optimum. Interestingly, when Berthoz et al. (2013) analysed what caused the path tracking optimum for human drivers in their study, this type of trajectory phase alignment is exactly what they found (see their Fig. 10). In our model, the reason this is happening is that the more the model underestimates its own yaw rate, the earlier and the more vigorously it will respond to the next turn in the slalom, causing the trajectory to reach apex earlier. This explanation also aligns with the analysis of steering angles by Feenstra et al. (2010, Fig. 4b; also reproduced as Fig. 6 in Berthoz et al., 2013), who found that when motion cues were absent, drivers adjusted their steering more quickly after passing a cone gate. This empirical finding matches what is seen in Fig. 9 here, and is indeed what one would expect from a driver who perceives that s/he isn't rotating quickly enough in preparation for the next cone gate.

In sum, from a path-tracking perspective the model captures essentially all aspects of what has been empirically established with respect to the sub-unity optimum phenomenon: Not only the existence of an optimum, but also its cause being trajectory phase alignment, as well as how the optimum is affected by slalom difficulty (Fig. 8a). Overall, this can be taken to suggest that underestimation of yaw rate (or, as said before, behaving *as if* one underestimates yaw rate) may indeed be the mechanism behind this phenomenon also in humans.

However, it should be noted that the local optimum in motion scaling has been observed also in subjective ratings of various types, and not necessarily at the exact same $\alpha$ as the path-tracking optimum (Berthoz et al., 2013; Savona et al., 2014). While the present model simulations can *possibly* help explain why there might be a local optimum in subjective ratings of for example "ease of completing the task" or similar, it seems less clear how the yaw rate underestimation mechanism would contribute to improved subjective ratings of for example realism. One possibility is of course that several mechanisms are in play here; the yaw rate underestimation mechanism might coexist with any and all of the mechanisms reviewed above in this section.

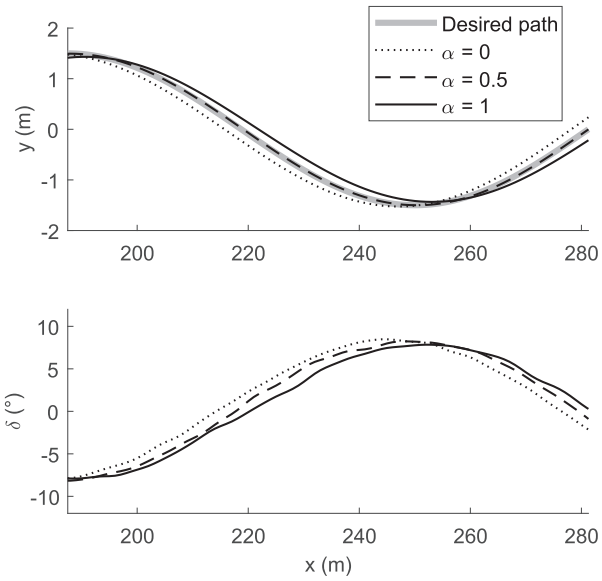


**Fig. 9.** The effect of motion scale factor $\alpha$ on the phase of model steering $\delta$ and resulting vehicle lateral position $y$, across a longitudinal subset of the simulated slalom track. The plotted traces are averages across twenty model simulations for each motion scale factor. The top and bottom panels can be compared to Figs. 10 and 6, respectively, in (Berthoz et al., 2013). The model used here is the intermittent control model, without any behavioural adaptation to the motion down-scaling. The vestibular noise was set to $\sigma_{ves} = 1^\circ/s = 2 \cdot \sigma_{vis}$, resulting in the path-tracking optimum occurring at $\alpha = 0.5$, as in the Berthoz et al. (2013) figure.

Another question raised by the present analyses is to what extent the sub-unity motion scaling optimum phenomenon is particular to slalom tasks. The phase-alignment path-tracking benefit from yaw rate underestimation observed here seems to be rather closely related to the specific nature of this task, such that it might not necessarily generalise.

### 4.3. Driver steering modelling

We have shown in this paper how the intermittent control framework of Markkula et al. (2018a) can be naturally extended to account for multisensory integration and a number of behavioural adaptation mechanisms; these extensions should be of value in a range of contexts relating to driving simulators and in other application domains.

It is notable, however, that much of the results of the intermittent control model were reproduced also by the continuous model. The main differences, quite expectedly, related to steering effort: In addition to the lack of the putatively effort-related evidence accumulation gain adaptation, which cannot be included in the continuous model, the effect of motion scaling on steering costs all but disappeared with all behavioural adaptations in the continuous model. Nevertheless, since the continuous model is so simple and easy to implement (just the few operations in the left part of Fig. 2 plus a delay and a gain), it seems particularly well suited for use in future studies of multisensory integration in driving simulators.

One limitation of all of the models tested here is that they rely on single point preview. While, as mentioned above, this type of model has been shown to capture many aspects of human steering, Boer (2016) has shown that it cannot replicate certain more advanced, anticipatory human behaviours, such as a "swing wide" before the first cone gate in a slalom, as an early preparation for the *second* cone gate. However, this type of behaviour does not seem central to our main findings here (regarding effects of motion down-scaling, the sub-unity tracking optimum, and behavioural adaptation mechanisms), since our findings arguably primarily concern the later, "steady state" oscillatory stage of the slalom.

The main alternative to the models tested here is the one proposed by Nash and Cole (2017). This model assumes optimal control in a more complete sense, with access to explicit internal models of the vehicle as well as of the sensory and neuromuscular dynamics. On a cursory analysis, it seems likely that also this model would exhibit lower performance and higher steering effort when motion is scaled down or turned off. Among the adaptation mechanisms studied here, the combined rescaling and reweighting mechanism (B) would seem to fit especially naturally within the framework. Here, the model behaviour with this mechanism did not align well with the existing empirical findings, but direct testing in model simulation would be needed to see whether it fares better in the Nash and Cole (2017) framework. Also the pure cue reweighting adaptation (A) could be used, if the optimal control framework is extended with a similar prediction-based estimation of reliabilities as proposed here. However, the gain adaptations (C) and (D) do not seem readily compatible with the Nash and Cole (2017) model.

It would also be interesting to test whether the Nash and Cole (2017) model reproduces the sub-unity motion scaling optimum phenomenon. At least in its non-adapted form, this model should also underestimate yaw rate. However, as discussed above, an important part of the reason why our model tracks the desired path better when underestimating yaw rate

is because with full motion cues its control is to a certain degree inherently suboptimal (the trajectory phase misalignment), something which, *a priori*, would not seem to be the case for the Nash and Cole (2017) model.

### 4.4. Future work

As has already been hinted at above, one obvious future direction would be to apply the models proposed here to other tasks besides the slalom. Ideally, one would first generate predictions for these other tasks using the model (perhaps just the continuous version of it, for simplicity), and then investigate whether these predictions are borne out in tests with human drivers. In such empirical work, one could also study the adaptation process itself in more detail, for example to try to distinguish better between the various hypothesised mechanisms for adaptation. Additional adaptation mechanisms are also imaginable. For example, it is possible that drivers respond to down-scaled or otherwise imperfect motion cues by adjusting the overall goals of their driving, something which could be operationalised in the present model as modifications to the cost function weights ($k_{\text{path}}$ and $k_{\text{steer}}$), or even Eq. (5) itself.

The model proposed here could also be applied in development and tuning of motion cueing algorithms, in its present form especially for direct scaling cueing. For example, one could use the model to predict what motion scaling might yield behaviour that is as similar as possible to that in a real vehicle, or to predict how large the differences might be between behaviour before and after adaptation to a certain motion scaling, to get an idea of what motion cueing settings might take longer time to get used to.

If the model is to be used with more complex, arbitrary motion cueing algorithms, for example affecting rotations and translations in different ways, the current simplified approach of capturing all vestibular sensing in just a yaw rate estimate will not be enough, and it needs to be better considered how different types of motion cues are used by drivers when determining the needed steering control. One possibility is the Nash and Cole (2017) approach, with sensory dynamics models and inverse model state estimators (modelling scheme (c) in Fig. 1). A possible complication here is that empirical observations suggest that rotation and translation cues may not be used by human drivers in precisely the ways suggested by this type of engineering analysis (Lakerveld et al., 2016).

## 5. Conclusion

We aimed to study visual-vestibular integration and behavioural adaptation in the driving simulator, by modelling human steering behaviour in slalom driving, a type of task that has been much studied in simulators with linearly down-scaled motion cues. To this end, we started from an existing modelling framework for intermittent sensorimotor control, building on concepts such as sensory evidence accumulation, motor primitives, and sensory predictions (corollary discharge), and extended it with mechanisms for optimal sensory cue integration and behavioural adaptation. The resulting extended framework, as well as a simplified continuous version of it, seem well suited for future work on multisensory integration and behavioural adaptation in driving simulators and elsewhere.

A key insight from the present work is that much of the empirically observed phenomena in motion down-scaling of slalom driving tasks can be explained by a *yaw rate underestimation* mechanism, whereby drivers respond to down-scaled simulator motion as if they perceived themselves and the simulated vehicle to be rotating more slowly than is the case in the simulated situation. This mechanism explains not only why removing motion cues leads to increased steering efforts and worse path tracking, but also captures a phenomenon for which there has previously been no good explanation: In an intermediate range of mild down-scaling, the yaw rate underestimation phenomenon counteracts an inherent suboptimality in the model's steering behaviour, resulting in improved path tracking.

A range of neurobiologically plausible mechanisms for behavioural adaptation were hypothesised and tested. Out of these, the only one that did not provide behavioural changes in line with the existing empirical literature was a compensatory rescaling of the vestibular input (to optimally counteract the motion down-scaling). The results instead suggest that empirically observed improvements over time, in prolonged task performance with down-scaled cues, may be achieved by human drivers by increasing gains in sensory evidence accumulation or steering response, and/or by detecting deviations between actual vestibular input and internal predictions of the same, and then using these deviations to determine how to down-weight the vestibular cues in the optimal cue integration scheme.

## Acknowledgment

This work was supported by Jaguar Land Rover and the UK-EPSRC Grant EP/K014145/1 as part of the jointly funded Programme for Simulation Innovation (PSi).

## Software and data

The software code implementing the models, simulations, and figures reported here is available at https://dx.doi.org/10.17605/OSF.IO/K6WCP. There are no primary research data associated with this paper; as should be clear from the text, all of the comparisons to human behaviour refer to empirical findings reported in previous literature.

## References


Aston-Jones, G., & Cohen, J. D. (2005). An integrative theory of locus coeruleus-norepinephrine function: Adaptive gain and optimal performance. *Annual Review of Neuroscience, 28*, 403–450.

Benderius, O., & Markkula, G. (2014). Evidence for a fundamental property of steering. *Proceedings of the human factors and ergonomics society annual meeting* (Vol. 58, pp. 884–888). .

Berthoz, A., Bles, W., Bülthoff, H. H., Correia Grácio, B. J., Feenstra, P., Filliard, N., ... Wentink, M (2013). Motion scaling for high-performance driving simulators. *IEEE Transactions on Human-Machine Systems, 43*(3), 265–276.

Boer, E. R. (2016). What preview elements do drivers need? *IFAC-PapersOnLine, 49*(19), 102–107.

Bogacz, R. (2017). A tutorial on the free-energy framework for modelling perception and learning. *Journal of Mathematical Psychology, 76*, 198–211.

Correia Grácio, B., Wentink, M., Valente Pais, A., Van Paassen, M., & Mulder, M. (2011). Driver behavior comparison between static and dynamic simulation for advanced driving maneuvers. *Presence: Teleoperators and Virtual Environments, 20*(2), 143–161.

Crapse, T. B., & Sommer, M. A. (2008). Corollary discharge circuits in the primate brain. *Current Opinion in Neurobiology, 18*, 552–557.

Feenstra, P., van der Horst, R., Grácio, B., & Wentink, M. (2010). Effect of simulator motion cuing on steering control performance: Driving simulator study. *Transportation Research Record: Journal of the Transportation Research Board, 2185*, 48–54.

Fetsch, C. R., DeAngelis, G. C., & Angelaki, D. E. (2013). Bridging the gap between theories of sensory cue integration and the physiology of multisensory neurons. *Nature Reviews Neuroscience, 14*(6), 429.

Fischer, M., Seefried, A., & Seehof, C. (2016). Objective motion cueing test for driving simulators. In *Proceedings of the driving simulation conference* (pp. 41–50).

Fisher, D. L., Rizzo, M., Caird, J. K., & Lee, J. D. (2011). *Handbook of driving simulation for engineering, medicine, and psychology*. Boca Raton, FL: CRC Press.

Franklin, D., & Wolpert, D. (2011). Computational mechanisms of sensorimotor control. *Neuron, 72*, 425–442.

Friston, K. (2005). A theory of cortical responses. *Philosophical Transactions of the Royal Society of London B: Biological Sciences, 360*(1456), 815–836.

Giszter, S. F. (2015). Motor primitives — New data and future questions. *Current Opinion in Neurobiology, 33*, 156–165.

Gold, J. I., & Shadlen, M. N. (2007). The neural basis of decision making. *Annual Review of Neuroscience, 30*, 535–574.

Gordon, T., & Magnuski, N. (2006). Modeling normal driving as a collision avoidance process. In *Proceedings of the 8th international symposium on advanced vehicle control*. .

Gordon, T., & Zhang, Y. (2015). Steering pulse model for vehicle lane keeping. In *Proceedings of 2015 IEEE international conference on computational intelligence and virtual environments for measurement systems and applications (CIVEMSA)*. .

Greenberg, J., Artz, B., & Cathey, L. (2003). The effect of lateral motion cues during simulated driving. In *Proceedings of the driving simulation conference North America*. .

Hosman, R. J. A. W. (1996). *Pilot's perception and control of aircraft motions* (Ph.D. thesis). TU Delft.

Jamson, A. H. J. (2010). *Motion cueing in driving simulators for research applications* (Ph.D. thesis). University of Leeds.

Johns, T. A., & Cole, D. J. (2015). Measurement and mathematical model of a driver's intermittent compensatory steering control. *Vehicle System Dynamics, 53*(12), 1811–1829.

Lakerveld, P., Damveld, H., Pool, D., van der El, K., van Paassen, M., & Mulder, M. (2016). The effects of yaw and sway motion cues in curve driving simulation. *IFAC-PapersOnLine, 49*(19), 500–505.

Lappi, O. (2014). Future path and tangent point models in the visual control of locomotion in curve driving. *Journal of Vision, 14*(12).

Markkula, G. (2013). *Evaluating vehicle stability support systems by measuring, analyzing, and modeling driver behavior* (Licentiate thesis). Chalmers University of Technology.

Markkula, G., Benderius, O., & Wahde, M. (2014). Comparing and validating models of driver steering behaviour in collision avoidance and vehicle stabilization. *Vehicle System Dynamics, 52*(12), 1658–1680.

Markkula, G., Boer, E., Romano, R., & Merat, N. (2018). Sustained sensorimotor control as intermittent decisions about prediction errors: Computational framework and application to ground vehicle steering. *Biological Cybernetics, 112*(3), 181–207.

Markkula, G., Romano, R., Jamson, A. H., Pariota, L., Bean, A., & Boer, E. R. (2018). Using driver control models to understand and evaluate behavioural validity of driving simulators. *IEEE Transactions on Human-Machine Systems, 48*(6), 592–603.

Mulder, M., Zaal, P., Pool, D. M., Damveld, H. J., & van Paassen, M. (2013). A cybernetic approach to assess simulator fidelity: Looking back and looking forward. In *AIAA modeling and simulation technologies conference*. .

Nash, C. J., & Cole, D. J. (2017). Modelling the influence of sensory dynamics on linear and nonlinear driver steering control. *Vehicle System Dynamics, 56*(5), 689–718.

Nash, C. J., Cole, D. J., & Bigler, R. S. (2016). A review of human sensory dynamics for application to models of driver steering and speed control. *Biological Cybernetics, 110*(2–3), 91–116.

Nesti, A., Beykirch, K. A., Pretto, P., & Bülthoff, H. H. (2015). Self-motion sensitivity to visual yaw rotations in humans. *Experimental Brain Research, 233*(3), 861–869.

Plochl, M., & Edelmann, J. (2007). Driver models in automobile dynamics application. *Vehicle System Dynamics, 45*(7–8), 699–741.

Purcell, B. A., Heitz, R. P., Cohen, J. Y., Schall, J. D., Logan, G. D., & Palmeri, T. J. (2010). Neurally constrained modeling of perceptual decision making. *Psychological Review, 117*(4), 1113–1143.

Ratcliff, R., Smith, P. L., Brown, S. D., & McKoon, G. (2016). Diffusion decision model: Current issues and history. *Trends in Cognitive Sciences, 20*(4), 260–281.

Repa, B. S., Leucht, P. M., & Wierwille, W. W. (1982). The effect of simulator motion on driver performance. Technical Paper 820307. SAE.

Requarth, T., & Sawtell, N. B. (2014). Plastic corollary discharge predicts sensory consequences of movements in a cerebellum-like circuit. *Neuron, 82*, 896–907.

Riemersma, J. (1981). Visual control during straight road driving. *Acta Psychologica, 48*(1–3), 215–225.

Salisbury, I., & Limebeer, D. (2017). Motion cueing in high-performance vehicle simulators. *Vehicle System Dynamics, 55*(6), 775–801.

Savona, F., Stratulat, A. M., Diaz, E., Honnet, V., Houze, G., Vars, P., ... Bourdin, C. (2014). The influence of lateral, roll, and yaw motion gains on driving performance on an advanced dynamic simulator. In *Proceedings of the sixth international conference on advances in system simulation* (pp. 113–119).

Siegler, I., Reymond, G., Kemeny, A., & Berthoz, A. (2001). Sensorimotor integration in a driving simulator: Contributions of motion cueing in elementary driving tasks. In *Proceedings of the driving simulation conference* (pp. 21–32).

Soyka, F., Giordano, P. R., Barnett-Cowan, M., & Bülthoff, H. H. (2012). Modeling direction discrimination thresholds for yaw rotations around an earth-vertical axis for arbitrary motion profiles. *Experimental Brain Research, 220*(1), 89–99.

Steen, J., Damveld, H. J., Happee, R., van Paassen, M. M., & Mulder, M. (2011). A review of visual driver models for system identification purposes. In *Proceedings of the 2011 IEEE international conference on systems, man, and cybernetics (SMC)*. .

Tan, H.-S., & Huang, J. (2012). Experimental development of a new target and control driver steering model based on dlc test data. *IEEE Transactions on Intelligent Transportation Systems, 13*(1), 375–384.

van Beers, R. J., Baraduc, P., & Wolpert, D. M. (2002). Role of uncertainty in sensorimotor control. *Philosophical Transactions of the Royal Society of London B: Biological Sciences, 357*(1424), 1137–1145.

van der Kooij, H., Jacobs, R., Koopman, B., & Grootenboer, H. (1999). A multisensory integration model of human stance control. *Biological Cybernetics, 80*(5), 299–308.

Wilkie, R. M., & Wann, J. P. (2005). The role of visual and nonvisual information in the control of locomotion. *Journal of Experimental Psychology: Human Perception and Performance, 31*(5), 901–911.

Zaal, P. M. T., Pool, D. M., Chu, Q. P., Mulder, M., Van Paassen, M. M., & Mulder, J. A. (2009). Modeling human multimodal perception and control using genetic maximum likelihood estimation. *Journal of Guidance, Control, and Dynamics, 32*(4), 1089–1099.